Original Article

J Babol Univ Med Sci
22; 2020. P: 195-202

Enhancing the Accuracy of Vascular Embolism Volumetry Using Medical Imaging Software

S.F. Ayatifard (MSc)[1], M. Pezeshkirad (MD)[2], M. Amini (MD)[3], N. Morovatdar (PhD)[4], J. Pirayesh Islamian (PhD)[*5]

1.Department of Medical Physics, Faculty of Medicine, Tabriz University of Medical Sciences, Tabriz, I.R.Iran
2.Department of Radiology, School of Medicine, Mashhad University of Medical Sciences, Mashhad, I.R.Iran
3.Department of Internal Medicine, School of Medicine, Mashhad University of Medical Sciences, Mashhad, I.R.Iran
4.Department of Community Medicine, School of Medicine, Mashhad University of Medical Sciences, Mashhad, I.R.Iran
5.Immunology Research Center, Tabriz University of Medical Sciences, Tabriz, I.R.Iran

J Babol Univ Med Sci; 22; 2020; PP: 195-202
Received: Jul 21st 2019, Revised: Oct 13rd 2019, Accepted: Oct 22nd 2019.

ABSTRACT

BACKGROUND AND OBJECTIVE: Detecting and accurate determining of vascular embolism dimensions are considered as a challenging issue in CT imaging. Present study aimed to enhance the accuracy of vascular embolism volumetry in managing a proper diagnosis and treatment of the disease.

METHODS: In this non experimental quantitative study, firstly we simulated coronary and aorta arteries with normal dimensions in a 4D extended NURBS based cardiac-torso phantom in a matrix sizes of 512×512 with slice thickness of 0.116 mm. Then, twenty five venous thromboembolisms with the diameters ranged 0.1-5 and 5-20 mm were created in the coronary arteries and aorta of the Phantom, respectively. The Medical Imaging Interaction Toolkit was used for localization and volume measurement of the produced venous thromboembolisms on the CT images. Finally, Accuracy of the measured data was compared with the simulated measures in the phantom.

FINDINGS: The difference on measures with the software was obtained 0.03±0.021 for embolies less than 4.64 mm (0.1 ml), (r=0.67, p=0.02), and 0.02±0.008 mm for embolies greater than 4.64 mm (r=0.99, p<0.001).

CONCLUSION: According to the acceptable volumetry accuracy of Medical Imaging Interaction Toolkit especially for volumes greater than 0.1 ml, may be used for an accurate thromboembolism and pulmonary embolism measurements.

KEY WORDS: *Embolism, Volumetry, Medical Diagnosis, Coronary Vessels, Aorta*.

Please cite this article as follows:

Ayatifard SF, Pezeshkirad M, Amini M, Morovatdar N, Pirayesh Islamian J. Enhancing the Accuracy of Vascular Embolism Volumetry Using Medical Imaging Software. J Babol Univ Med Sci. 2020; 22: 195-202.

***Corresonding Author: J. Pirayesh Islamian (PhD)**
Address: Department of Medical Physics, Faculty of Medicine, Tabriz University of Medical Sciences, Tabriz, I.R.Iran
Tel: +98 41 33364660
E-mail: pirayeshj@tbzmed.ac.ir

[DOR: 20.1001.1.15614107.1399.22.1.26.8]
[DOI: 10.22088/jbums.22.1.195]

Introduction

Venous Thromboembolism (VTE), including deep vein thrombosis (DVT) and pulmonary embolism (PE), is the most common cause of preventable death (1-4). The death rate is 1.73 per year per 100,000 people due to acute pulmonary embolism in Australia and New Zealand (5). Clinical signs in the diagnosis of pulmonary embolism alone have a sensitivity of 85% and a specificity of 51% (6). Coronary embolism has been one of the death causes in acute coronary syndrome (7).

Among diagnostic methods, computed tomography with contrast material is the main imaging method for pulmonary embolism (8-13). Spiral CT scans can take pictures of the chest area in 1 mm incisions. In suspected cases of PE, computed tomography pulmonary angiography (CTPA) is performed because of its accuracy, speed, cross-sectional reconstruction, and differential diagnosis (9,14,15). An embolism is defined as a defect in the filling of the contrast medium in the non-contrast medium by convexity towards the proximal of the vascular duct (16).

Miller, Walsh, Qanadli, and Masotra grading methods are semi-quantitative methods for determining the extent of vascular embolism (5,9,17,18). The difference between these grades in grading is the location of the clot and the arteries branching from it, the extent of the blockage and the length of the clot. Furlan et al. studied the relationship between acute pulmonary embolism mortality and clot load with the help of Qanadli and Masotra semi-quantitative grades and semi-right cardiac dysfunction in pulmonary CTA. The volume of the clot estimated by the proprietary software on the CT scan device was strongly related to the clot load and a larger clot volume was consistent with a higher incidence of right heart failure (18).

Lim et al. reported the sensitivity and specificity of spiral CT scan in determining the size of the right ventricle following acute pulmonary embolism, 91.6% and 100%, respectively (19). So far, no high-precision validation method has been proposed for quantitative calculation of clot volume. There are software for display, analysis, digital computing, format conversion, processing, reconstruction and various dimensional measurements that can be used in this regard after validation using CT and MRI images (20-26). In this regard, Utku et al. to reconstruct CT-scan imaging with 3 mm chest incisions with 512×512 and 12-bit three-dimensional matrix and the anatomical size of aortic aneurysms measurements, introduced Aortic Aneurysm Measurement and Evaluation Tool (AMET) as an aortic aneurysm measurement and evaluation software to optimize the improvement of treatment strategy and effective disease management (27).

Bendtsen et al., using the Definiens XD platform program in tumor measurement, suggested that instead of examining the length of the tumor, use tumor volume to better manage lung cancer treatment (28). Behnia et al., in assessing the accuracy of measuring the thickness of the labial and palatal bones to the maxillary anterior teeth by Cone Beam Computed Tomography (CBCT) method, reliable accuracy for obtaining measurements of the labial bone thickness above 1 mm (29). Cai et al., used the Medical Imaging ToolKit (MITK) segmentation method to determine the exact contour of the liver in CT-scan imaging to compare semi-automated and automated volumetric approaches (30).

The XCAT phantom (4D Extended NURBS based Cardiac-Torso human phantom) was commonly used in Monte Carlo simulation studies, due to its complete adaptation to the geometric image and the weakening of body organs (31). Pirayesh Islamian et al., used this phantom with a myocardial deficiency to evaluate the quality of SPECT images by Monte Carlo SIMIND code (32). Also, Khoshakhlagh evaluated this phantom by using hot and cold lesions in the liver to investigate the effect of SPECT on the ability to detect hot and cold liver lesions (33). Therefore, the present study was performed to evaluate the accuracy of MITK in XCAT phantom vascular embolism images.

Methods

This quantitative non-experimental study was approved by the Institutional Ethics Committee of Tabriz University of Medical Sciences (TBZMED.REC.1394.53). Coronary and aortic artery clot volume was measured by creating 25 vascular clots (test variable) with dimensions (measurement criteria) of 0.1 to 20 mm in XCAT human phantom vessels (27) (512×512 matrices and slice thickness of 0.116 mm), using MITK software. The imageJ (34) program version p1.44 was used to attach the clot to the coronary arteries (beginning of the right coronary artery-RCA1) and the XCAT phantom aorta (Figure 1). To import phantom files (.bin) into MITK software, using XmedCon (35) software version 0.10.5, the files were converted to readable MITK format (.nii files). For volumetric measurement, XCAT phantom scan images (containing vascular clots) were examined for clot volume in all axial sections using MITK software version 1.1 in the Segmentation section. In this program, the pixels related to embolism were colored individually, and finally, the sum of the pixels was determined in milliliters. The above steps were conducted separately for each of the 25 clot phantoms located in the coronary artery and aorta (Figure 2) (24,25). In order to statistically analyze the data, the SPSS software version 16 was used. For this purpose, the Kolmogorov-Smirnov test was used to compare the studied parameters in terms of data normality. Pearson correlation coefficient and the Intraclass correlation coefficient were used to evaluate the level of correlation and agreement between embolism volume designed in Phantom XCAT and calculated by MITK software. Scatter diagram and Bland–Altman plots were used to present the results and p<0.05 was considered statistically significant.

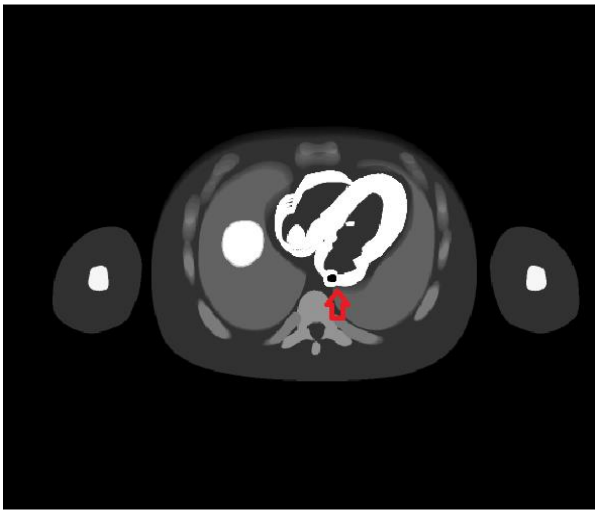

Figure 1. XCAT chest phantom transects image simulated. A 17 mm diameter clot forms in the aorta (red arrow)

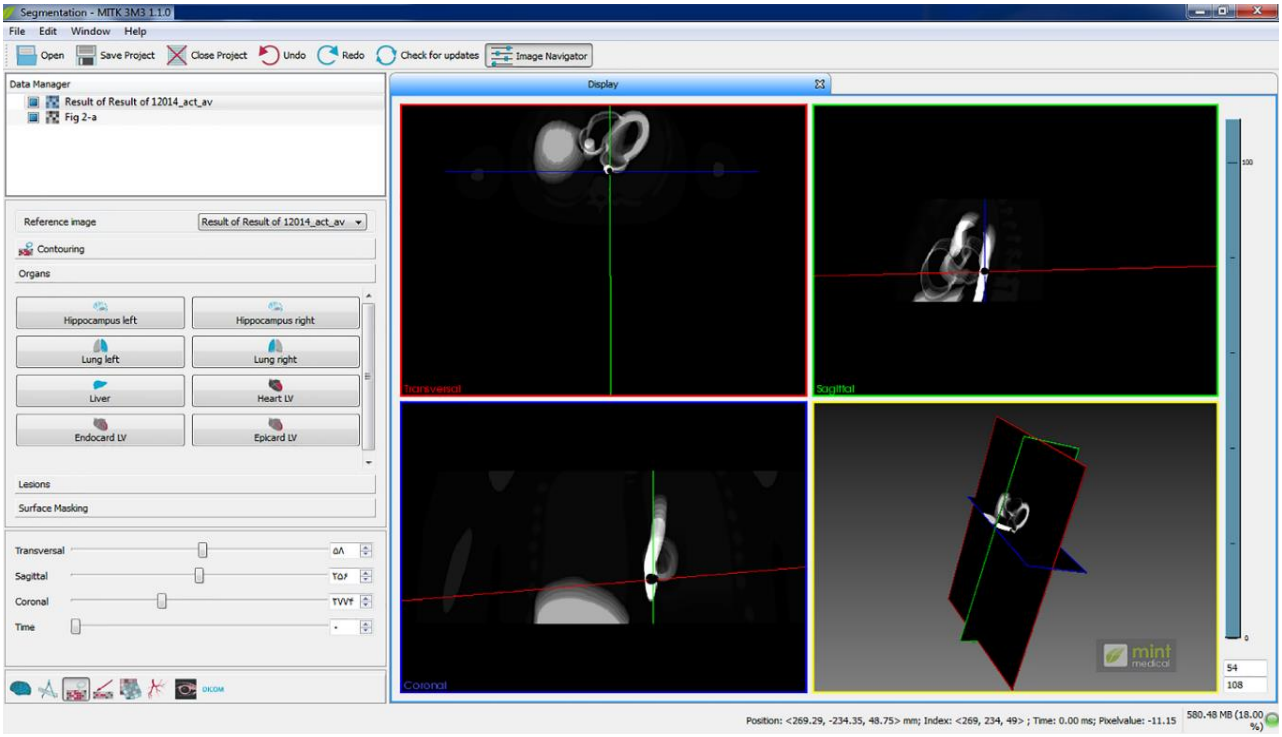

Figure 2. Screenshot of an XCAT phantom heart scan containing a clot in the descending aortic artery at the axial trans (top left), sagittal (top right), and coronal (bottom left) sections in the MITK program

Results

In the present study, volumetric measurements were conducted for vascular clots with a volume of 0.002 to 3.3 ml using MITK software. XCAT-designed embolism volume data and MITK-measured embolism volume data showed that coronary artery clots with a diameter of 0.1 to 5 mm (p= 0.02, r= 0.67) and descending aortic artery clots 6 to 20 mm diameters (p<0.001, r= 0.99) can be accurately measured with MITK software (Table 1). The difference between the volume of fewer than 0.1 ml of embolism volume designed by XCAT and the volume of embolism measured by MITK does not matter in the clinic and was studied only to determine the minimum volume that can be measured by MITK, due to the very small range of clot volume. However, at volumes above 0.1 ml (normal volume in clinical use), embolic volume values designed with XCAT and measured with MITK showed acceptable accommodation. MITK software for calculating volumes of clots with a minimum volume of 0.1 ml showed high accuracy and acceptable error with intergroup correlation coefficient (ICC) test ($p<0.001$, $r= 0.98$) (Figure 3).

Results of the accuracy of volumetric adaptation of vascular clots with a diameter of 0.1-20 mm in the human phantom XCAT using MITK software to measure the software difference for clots with a diameter of less than 4.64 mm (volume 0.1 ml), 0.0±3.021 ($p= 0.02$, $r= 0.67$) and for clots with a diameter above 4.64 mm, the difference was 0.02±0.008 mm ($p< 0.001$, $r= 0.99$). In Figures 4 and 5, the results show the degree of conformity of the measurement with the actual value in the coronary arteries (actual clot diameter 0.1 to 5 mm in phantom coronary arteries) and the aorta (actual clot diameter 6 to 20 mm in the descending aorta) phantom is presented, respectively.

Table 1. Vascular clot volumetric data in coronary arteries and aorta of XCAT phantom with MITK software

	Volume of embolism (ml)		P-value
	Actual volume with XCAT	Measured with MITK	
Coronary clot (0.1-5 mm)	0.002	0	0.02
	0.004	0	
	0.02	0	
	0.04	0.1	
	0.066	0.1	
	0.086	0.1	
	0.1	0.1	
Aortic clot (6-20 mm)	0.09	0.1	<0.001
	0.143	0.1	
	0.214	0.2	
	0.304	0.3	
	0.418	0.4	
	0.666	0.6	
	0.722	0.7	
	0.918	0.9	
	1.146	1.2	
	1.472	1.6	
	1.714	1.7	
	2.066	2.1	
	2.441	2.4	
	2.870	2.9	
	3.3448	3.3	

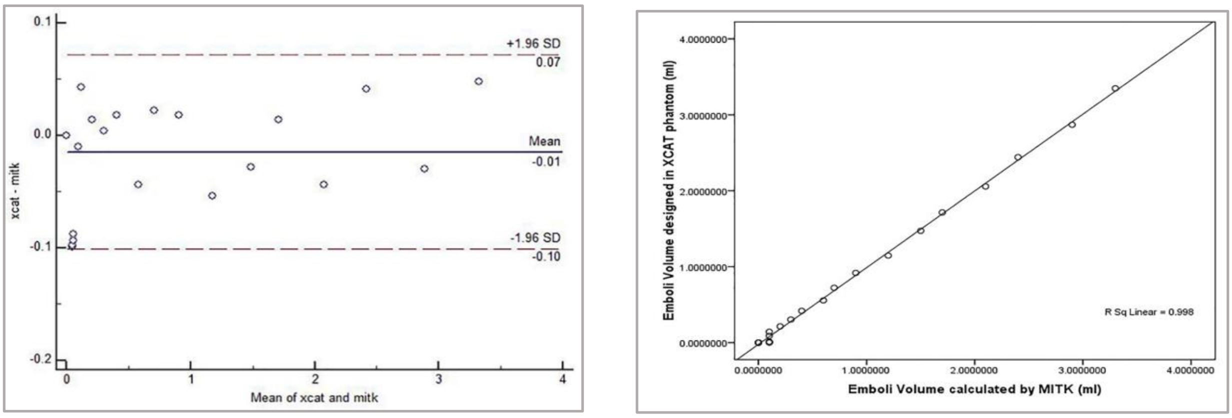

(3-A) **(3-B)**

Figure 3. Diagram of the results of matching embolism volume values (0.1–20 mm in diameter) designed in the coronary arteries and aorta of XCAT phantoms and measured with MITK (A: Bland-Altman plots, B: Scatter plot)

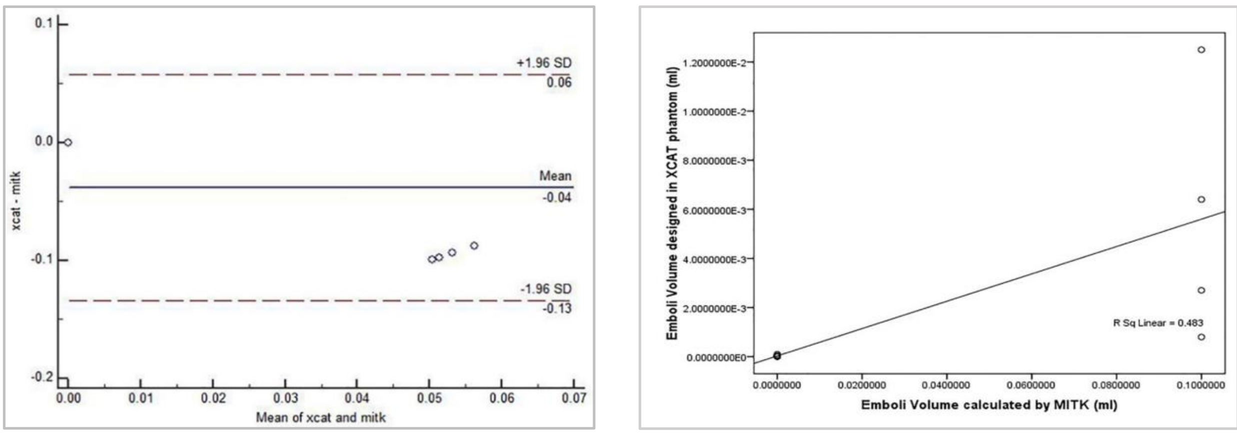

(4-A) **(4-B)**

Figure 4. Diagram of the results of matching embolism volume values (0.1–20 mm in diameter) in the coronary arteries of XCAT phantoms and measured with MITK (A: Bland–Altman plots, B: Scatter plot)

[DOI: 10.22088/jbums.22.1.195]
[DOR: 20.1001.1.15614107.1399.22.1.26.8]

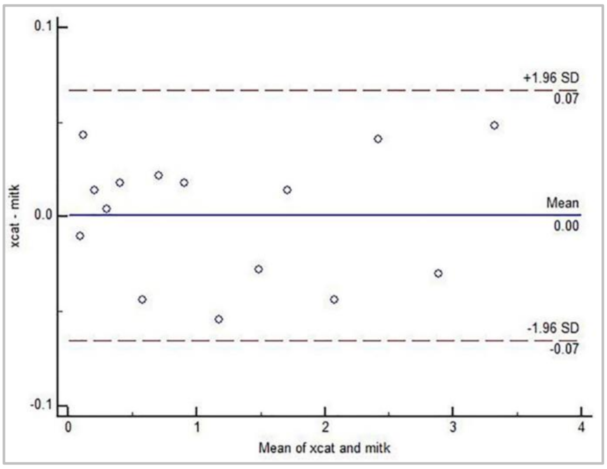

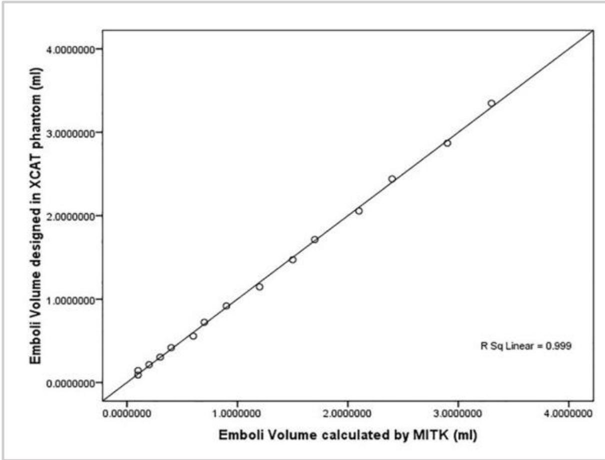

(5-A) **(5-B)**

Figure 5. Diagram of the results of matching embolism volume values (6-20 mm in diameter) in the aortic artery of Phantom XCAT and measured with MITK (A: Bland–Altman plots, B: Scatter plot)

Discussion

Association of the data of the present study showed the difference in measurement of MITK software for clots with a diameter of less than 4.64 mm (volume 0.1 ml), 0.03±0.021 ($p= 0.02$, $r= 0.67$) and for clots with a diameter above 4.64 mm, the difference of 0.02±0.008 mm ($p<0.001$, $r= 0.99$) was determined in XCAT phantom. Due to the importance of embolism and the lack of a reliable method for obtaining embolism volume, the present study proves the acceptable accuracy of MITK software in determining clot volume above 0.1 ml with acceptable accuracy and quantitative measurement of thromboembolism volume, a more accurate criterion provides for the diagnosis, treatment, and follow-up of PE and VTE patients and more accurate scoring. According to Bland-Altman plots and Scatter plot, 98% of accommodation was observed between the actual embolism volume in XCAT and the volume measured with MITK.

Furlan et al., study with physical phantom consisting of two polyester tubes containing contrast material and blood clot (the combination of blood and sodium citrate) for clot volume measurement by CT angiography and then using software of modified SRG method and statistical analysis of data by ICC method showed the difference in clot volume in the two methods was not significant (17).

Although the modified SRG method is a semi-automatic volumetric method that is determined by placing a spherical volume (sphere diameter assumption four and voxel) on the target area and averaging the Hounsfield numerical range, and by applying cluster growth processes, adjacent voxels spheres with this CT number range are volumetric. In the study of Behnia et al., which was conducted to evaluate the accuracy of the CBCT device, the thickness of the anterior and the palatal surface of the maxillary anterior teeth were measured with CBCT and compared with the extracted teeth. After comparison, it was found that this device is capable of measuring the thickness of above 1 mm (29).

Our study, while the software was independent of the CT scan, provided a measurable minimum volume of 0.1 ml. The advantage of being an independent image measuring tool, being portable, and not being dependent on the hardware of the imaging device, makes it possible to increase the admission of patients in the imaging department. For more accurate diagnosis and subsequent better disease management and follow-up, there are a variety of scoring methods for estimating the effect of embolic sizes, such as Miller, Walsh, Qanadli, and Mastora methods, which are semi-quantitative methods. The difference between these methods is in scoring the location of the clot and the subcranial arteries, the degree of obstruction, and the length of the clot.

The present study demonstrated the ability of the MITK program to determine and estimate vascular clot volume with acceptable accuracy as a completely quantitative factor with the human digital phantom. Therefore, due to the acceptable accuracy of volume measurement, especially in volumes above 0.1 ml, it can be used in the measurement of VTE and PE. Increasing patient admission, reducing time and spending, with the possibility of operating a computer independent of the imaging system and thus proper management of diagnosis and treatment of embolism is provided by this software.

Acknowledgment

Here by we would like to thank the Immunology Research Center of Tabriz University of Medical Sciences for cooperation in this project.

References

1.Kazemi T, Qasemi M, Taghavi-shawazi M. Epidemiologic Study of Patients with DVT in Birjand Vali-E-Asr Hospital-(2009-2014): Short Communication. J Birjand Univ Med Sci. 2016;23(1):86-91. [In Persian]

2.Beckman MG, Hooper WC, Critchley SE, Ortel TL. Venous Thromboembolism: A Public Health Concern. Am J Prev Med. 2010;38(4 Suppl):S495-501.

3.Beckman MG, Abe K, Barnes K, Bartman B, Brady PJ, Hooper WC. Strategies and Partnerships Toward Prevention of Healthcare-Associated Venous Thromboembolism. J Hosp Med. 2016;11 (Suppl 2):S5-S7.

4.Lieberman JR, Heckmann N. Venous Thromboembolism Prophylaxis in Total Hip Arthroplasty and Total Knee Arthroplasty Patients: From Guidelines to Practice. J Am Acad Orthop Surg. 2017;25(12):789-98.

5.Hepburn-Brown M, Darvall J, Hammerschlag G. Acute pulmonary embolism: a concise review of diagnosis and management. Intern Med J. 2019;49(1):15-27.

6.Morrone D, Morrone V. Acute Pulmonary Embolism: Focus on the Clinical Picture. Korean Circ J. 2018;48(5):365-81.

7.Raphael CE, Heit JA, Reeder GS, Bois MC, Maleszewski JJ, Tilbury RT, et al. Coronary embolus: an underappreciated cause of acute coronary syndromes. JACC Cardiovasc Interv. 2018;11(2):172-180..

8.Konstantinides SV, Barco S, Lankeit M, Meyer G. Management of Pulmonary Embolism. J Am Coll Cardiol. 2016;67(8):976-90.

9.Gibson NS, Sohne M, Buller HR. Prognostic value of echocardiography and spiral computed tomography in patients with pulmonary embolism. Curr Opin Pulm Med. 2005;11(5):380-4.

10.Konstantinides SV, Torbicki A, Agnelli G, Danchin N, Fitzmaurice D, Galie N, et al. 2014 ESC guidelines on the diagnosis and management of acute pulmonary embolism. Eur Heart J. 2014;35(43):3033-69.

11.Dogan H, de Roos A, Geleijins J, Huisman MV, Kroft LJ. The role of computed tomography in the diagnosis of acute and chronic pulmonary embolism. Diagn Interv Radiol. 2015;21(4):307-16.

12.Kasper DL, Fauci AS, Hauser SL, Longo DL, Jameson JL, Loscalzo J. Harrison's principles of internal medicine, 19th ed. New York: McGraw Hill Education; 2015.

13.Leitman EM, McDermott S. Pulmonary arteries: imaging of pulmonary embolism and beyond. Cardiovasc Diagn Ther. 2019;9 (Suppl 1):S37-S58.

14.Melot C, Naeije R. Pulmonary Vascular Diseases. Compr Physiol. 2011;1(2):593-619.

15.Konstantinides SV, Meyer G, Becattini C, Bueno H, Geersing G-J, Harjola V-P, et al. 2019 ESC Guidelines for the diagnosis and management of acute pulmonary embolism developed in collaboration with the European Respiratory Society (ERS): The Task Force for the diagnosis and management of acute pulmonary embolism of the European Society of Cardiology (ESC). Eur Heart J. 2020;41(4):543-603.

16.PIOPED investigators. Value of the ventilation/perfusion scan in acute pulmonary embolism. Results of the prospective investigation of pulmonary embolism diagnosis (PIOPED). JAMA. 1990;263(20):2753-9.

17.Furlan A, Patil A, Park B, Chang C-CH, Roberts MS, Bae KT. Accuracy and reproducibility of blood clot burden quantification with pulmonary CT angiography. AJR Am J Roentgenol. 2011;196(3):516-23.

18.Furlan A, Aghayev A, Chang CC-H, Patil A, Jeon KN, Park B, et al. Short-term mortality in acute pulmonary embolism: clot burden and signs of right heart dysfunction at CT pulmonary angiography. Radiology. 2012;265(1): 283-93.

19.Lim K-E, Chan C-Y, Chu P-H, Hsu Y-Y, Hsu W-C. Right ventricular dysfunction secondary to acute massive pulmonary embolism detected by helical computed tomography pulmonary angiography. Clin Imaging. 2005;29(1): 16-21.

20.Medson K, Vargas-Paris R, Nordgren-Rogberg A, Sigbergsdottir A, Nyrén S, Lindholm P. Primary diagnosis of pulmonary embolism with unenhanced MRI for patients not eligible for CTPA: Clinical outcome. Eur J Radiol Open. 2019;6:315-9.

[DOR: 20.1001.1.15614107.1399.22.1.26.8]
[DOI: 10.22088/jbums.22.1.195]

21.Biglino G, Capelli C, Wray J, Schievano S, Leaver L-K, Khambadkone S, et al. 3D-manufactured patient-specific models of congenital heart defects for communication in clinical practice: feasibility and acceptability. BMJ Open. 2015;5(4):e007165.

22.Bicknell RDC, Klinkhamer AJ, Flavel RJ, Wroe S, Paterson JR. A 3D anatomical atlas of appendage musculature in the chelicerate arthropod Limulus polyphemus. PLOS ONE. 2018;13(2):e0191400.

23.Tinelli G, Hertault A, Martin Gonzalez T, Spear R, Azzaoui R, Sobocinski J, et al. Evaluation of a new imaging software for aortic endograft planning. Eur Rev Med Pharmacol Sci. 2017;21(11):2717-24.

24.Maleike D, Nolden M, Meinzer H-P, Wolf I. Interactive segmentation framework of the Medical Imaging Interaction Toolkit. Comput Meth Prog Biomed. 2009;96(1):72-83.

25.Nolden M, Zelzer S, Seitel A, Wald D, Muller M, Franz AM, et al. The Medical Imaging Interaction Toolkit: challenges and advances : 10 years of open-source development. Int J Comput Assist Radiol Surg. 2013;8(4):607-20.

26.Rosset A, Spadola L, Ratib O. OsiriX: an open-source software for navigating in multidimensional DICOM images. J Digit Imaging. 2004;17(3):205-16.

27.Utku S, Baysal H, Yilmaz R, Gulcu A, Kut RA, Goktay AY. Improved computerized evaluation of abdominal aortic aneurysm. Turk J Elec Eng & Comp Sci. 2012; 20(Sup.2):1408-24.

28.Bendtsen C, Kietzmann M, Korn R, Mozley PD, Schmidt G, Binnig G. X-Ray Computed Tomography: Semiautomated Volumetric Analysis of Late-Stage Lung Tumors as a Basis for Response Assessments. Int J Biomed Imaging. 2011;2011.

29.Behnia H, Motamedian SR, Kiani MT, Morad G, Khojasteh A. Accuracy and reliability of cone beam computed tomographic measurements of the bone labial and palatal to the maxillary anterior teeth. Int J Oral Maxillofac Implants. 2015;30(6):1249-55.

30.Cai W, He B, Fan Y, Fang C, Jia F. Comparison of liver volumetry on contrast-enhanced CT images: one semiautomatic and two automatic approaches. J Appl Clin Med Phys. 2016;17(6):118-27.

31.Segars WP, Sturgeon G, Mendonca S, Grimes J, Tsui BMW. 4D XCAT phantom for multimodality imaging research. Med Phys. 2010;37(9):4902-15.

32. Pirayesh Islamian J, Bahreyni Toossi MT, Momennezhad M, Zakavi SR, Sadeghi R, Ljungberg M. Monte carlo study of the effect of collimator thickness on T-99m source response in single photon emission computed tomography. World J Nucl Med. 2012;11(2):70-4.

33.Khoshakhlagh M, Pirayesh Islamian J, Abedi SM, Mahmoudian B, Shayesteh Azar M. A Monte Carlo study for optimizing the detector of SPECT imaging using a XCAT human phantom. Nucl Med Rev Cent East Eur. 2017;20(1): 10-4.

34.Schneider CA, Rasband WS, Eliceiri KW. NIH Image to ImageJ: 25 years of image analysis. Nat Methods. 2012;9(7):671-5.

35.Nolf E, Voet T, Jacobs F, Dierckx R, Lemahieu I. (X)MedCon * An OpenSource Medical Image Conversion Toolkit. Eur J Nucl Med Mol Imaging. 2003;30:S246.

[DOR: 20.1001.1.15614107.1399.22.1.26.8]
[DOI: 10.22088/jbums.22.1.195]